UC Irvine
UC Irvine Previously Published Works

Title

Accuracy and precision of ^{14}C-based source apportionment of organic and elemental carbon in aerosols using the Swiss_4S protocol

Permalink

Journal

Atmospheric Measurement Techniques, 8(9)

ISSN

1867-8548

Authors

Mouteva, G. O
Fahrni, S. M
Santos, G. M
et al.

Publication Date

2015-09-16

DOI

10.5194/amt-8-3729-2015

Peer reviewed

Atmospheric
Measurement
Techniques
Open Access

Accuracy and precision of ^{14}C-based source apportionment of organic and elemental carbon in aerosols using the Swiss_4S protocol

G. O. Mouteva[1], S. M. Fahrni[1,a], G. M. Santos[1], J. T. Randerson[1], Y.-L. Zhang[2], S. Szidat[2], and C. I. Czimczik[1]

[1]Earth System Science, University of California, Irvine, CA, USA
[2]Department of Chemistry and Biochemistry & Oeschger Centre for Climate Change Research, University of Bern, Bern, Switzerland
[a]now at: Eidgenössische Technische Hochschule (ETH), Zürich, Switzerland

Correspondence to: G. O. Mouteva (gmouteva@uci.edu)

Abstract. Aerosol source apportionment remains a critical challenge for understanding the transport and aging of aerosols, as well as for developing successful air pollution mitigation strategies. The contributions of fossil and non-fossil sources to organic carbon (OC) and elemental carbon (EC) in carbonaceous aerosols can be quantified by measuring the radiocarbon (^{14}C) content of each carbon fraction. However, the use of ^{14}C in studying OC and EC has been limited by technical challenges related to the physical separation of the two fractions and small sample sizes. There is no common procedure for OC/EC ^{14}C analysis, and uncertainty studies have largely focused on the precision of yields. Here, we quantified the uncertainty in ^{14}C measurement of aerosols associated with the isolation and analysis of each carbon fraction with the Swiss_4S thermal–optical analysis (TOA) protocol. We used an OC/EC analyzer (Sunset Laboratory Inc., OR, USA) coupled to a vacuum line to separate the two components. Each fraction was thermally desorbed and converted to carbon dioxide (CO_2) in pure oxygen (O_2). On average, 91 % of the evolving CO_2 was then cryogenically trapped on the vacuum line, reduced to filamentous graphite, and measured for its ^{14}C content via accelerator mass spectrometry (AMS). To test the accuracy of our setup, we quantified the total amount of extraneous carbon introduced during the TOA sample processing and graphitization as the sum of modern and fossil (^{14}C-depleted) carbon introduced during the analysis of fossil reference materials (adipic acid for OC and coal for EC) and contemporary standards (oxalic acid for OC and rice char for EC) as a function of sample size. We further tested our methodology by analyzing five ambient airborne particulate matter ($PM_{2.5}$) samples with a range of OC and EC concentrations and ^{14}C contents in an interlaboratory comparison. The total modern and fossil carbon blanks of our setup were 0.8 ± 0.4 and $0.67 \pm 0.34\,\mu g\,C$, respectively, based on multiple measurements of ultra-small samples. The extraction procedure (Swiss_4S protocol and cryo-trapping only) contributed $0.37 \pm 0.18\,\mu g$ of modern carbon and $0.13 \pm 0.07\,\mu g$ of fossil carbon to the total blank of our system, with consistent estimates obtained for the two laboratories. There was no difference in the background correction between the OC and EC fractions. Our setup allowed us to efficiently isolate and trap each carbon fraction with the Swiss_4S protocol and to perform ^{14}C analysis of ultra-small OC and EC samples with high accuracy and low ^{14}C blanks.

1 Introduction

Carbonaceous aerosols play an important role in the Earth system by influencing many biogeochemical and climate processes (Pöschl, 2005; Jimenez et al., 2009). By absorbing and scattering solar and terrestrial radiation, carbonaceous aerosols directly affect Earth's radiation budget (Andreae and Gelencsér, 2006). As cloud condensation nuclei, they influence cloud formation (Novakov and Penner 1993; Dusek et

al., 2006; Spracklen et al., 2011) and microclimate (Bond et al., 2013). Carbonaceous aerosols also affect atmospheric chemistry by reacting with photooxidants, such as ozone and nitrogen dioxide, and acids (Lary et al., 1997; Ammann et al., 1998).

Emissions of carbonaceous aerosols from fossil-fuel combustion and biomass burning have significantly increased since preindustrial times (Griffin and Goldberg, 1983; McConnel et al., 2007) and account for a major fraction of fine particulate matter in polluted urban environments and in the global atmosphere (Pöschl, 2005). Numerous studies show that high concentrations of fine air particulate matter are correlated with severe health effects, such as enhanced cardiovascular, respiratory and allergic diseases and mortality (Gauderman and Avol, 2004; Mauderly and Chow, 2008; Janssen et al., 2011; Johnston et al., 2012). Due to their direct and indirect effects on climate, as well as their strong influence on the air quality and human health, carbonaceous aerosols have become a major environmental concern worldwide.

Carbonaceous aerosols encompass all particles containing carbon, excluding carbonates. This highly variable mixture of compounds is traditionally divided in two fractions: weakly refractory, light polycyclic or polyacidic hydrocarbons (organic carbon, OC) and strongly refractory, highly polymerized and light-absorbing carbon (elemental or black carbon, EC) (Pöschl, 2005). Both fractions play decisive, yet very different roles in the global climate system. The two fractions also originate from distinct sources and undergo different aging processes (Pöschl, 2005; Hallquist et al., 2009; Jimenez et al., 2009; Szidat et al., 2009; Bond et al., 2013). Particulate OC originates from either primary (i.e., direct) emissions or secondary formation (i.e., by oxidation of volatile organic compounds (VOCs)), whereas EC derives from incomplete combustion of fossil fuels or biomass. Assessing the respective contribution of fossil and biomass burning emissions is necessary in many air quality and climate mitigation applications for the development of efficient abatement strategies (Penner et al., 2010; Zhang et al., 2012; Bond et al., 2013; Szidat et al., 2013).

One way to investigate the sources of OC and EC is to measure their radiocarbon (^{14}C) content. Radiocarbon is a naturally occurring radioisotope that is produced in the atmosphere by cosmic ray interaction with nitrogen gas. Radiocarbon is oxidized to carbon dioxide (CO_2) and enters the food chain through photosynthesis so that all living things are intrinsically labeled with a characteristic radiocarbon-to-carbon ratio ([14]C / [12]C). The carbon content of materials with [14]C / [12]C ratios similar to the present [14]C / [12]C ratio of atmospheric CO_2 is described as *modern*. As ^{14}C decays, [14]C / [12]C ratios approach zero, as compared to a modern standard ([14]C / [12]C$_{sample}$ $\ll$ [14]C / [12]C$_{standard}$), and the carbon content is then described as *fossil*. In addition to natural production of ^{14}C, atmospheric nuclear weapons testing produced large quantities of ^{14}C in the mid-20th century. Since the partial test cessation in 1963, atmospheric ^{14}C levels have been declining as this bomb-^{14}C is mixed with older CO_2 outgassing from the oceans and soils and is further diluted by increasing levels of emissions of fossil CO_2 (Levin et al., 2010). Thus, modern and fossil sources of OC and EC in carbonaceous aerosols can be quantified by measuring their ^{14}C content. For aerosols, biomass burning and organic aerosols derived from biogenic VOCs produce carbon with a modern ^{14}C signature, while fossil fuel combustion generates carbon depleted in [14]C (Clayton et al., 1955).

Since OC and EC fractions differ in their origins and often show very different ^{14}C signatures (Szidat et al., 2004, 2009), ^{14}C-based source apportionments require a clear and physical separation between OC and EC. However, there is no defined sharp boundary between OC and EC, but a continuous increase of thermochemical refractiveness and specific optical absorption going from non-refractive and colorless organic compounds to graphite-like structures (Pöschl, 2005). Further, OC can be pyrolized (charred) into EC during analytical procedures. Therefore, the OC/EC split is defined based on the applied optical or thermochemical methods used (absorption wavelength, temperature gradient, etc.), which can lead to substantially different results and strongly limits the comparability and suitability of OC and EC data for the determination of mass balances and physicochemical properties of aerosols.

Thermal–optical analysis (TOA) is one of the most commonly applied techniques for OC/EC measurements (Schmid et al., 2001; Chow et al., 2004; Cavalli et al., 2010). However, moderate changes in the thermal evolution protocol for an OC/EC analysis can have a large impact on the OC/EC split (Schauer et al., 2003). A protocol allowing the isolation of OC and EC for accurate ^{14}C measurements requires a complete removal of interfering fractions with maximum CO_2 recovery from each fraction. Recently, Zhang et al. (2012) developed such a TOA protocol ("Swiss_4S") with optimized thermal–optical conditions to minimize OC charring, untimely removal of EC, and the potential positive artifacts leading to co-evolution of EC with residual OC.

Here, we describe an investigation of the precision and accuracy of the Swiss_4S protocol for ^{14}C analysis of OC and EC using the W. M. Keck Carbon Cycle Accelerator Mass Spectrometry Laboratory (KCCAMS) at the University of California (UC), Irvine. We coupled a thermal–optical aerosol analyzer (OC/EC analyzer, Sunset Laboratory Inc., Portland, OR, USA), which oxidizes each fraction to CO_2, to a vacuum line, allowing us to cryogenically trap each fraction's CO_2 for ^{14}C analysis. We quantified the blank associated with our setup by analyzing both modern and fossil OC and EC standard materials ranging in size from 4 to 43 µg C. The goals of this study were to evaluate the performance of our analytical setup, quantify the uncertainties and compare the consistency of our results with those from the Laboratory of Radiochemistry and Environmental Chemistry at the University of Bern, Switzerland (Zhang et al., 2012). This study

is an important step towards developing a common procedure for the ^{14}C analysis of OC and EC in fine air particulate matter.

2 Methods and materials

To achieve precise and reproducible ^{14}C measurements of OC and EC aerosol carbon fractions, we performed three consecutive steps. First, we introduced a sample into a thermal–optical OC/EC analyzer coupled to a vacuum line. The aerosol carbon fraction of interest (either OC or EC) was isolated via the OC/EC analyzer with the Swiss_4S protocol and cryogenically trapped on the vacuum line in the form of CO_2 and sealed into a Pyrex tube. Second, we converted the CO_2 into a solid target (graphite) that was subsequently analyzed for its ^{14}C content with accelerator mass spectrometry (AMS). Samples were graphitized via hydrogen reduction, specifically optimized for small samples (Santos et al., 2007a). Third, the total uncertainty associated with OC/EC separation, cryo-trapping, graphitization and ^{14}C analysis was estimated as the sum of modern and fossil carbon contaminations. This information was used to adjust the fraction modern values of our samples (Santos et al., 2010). This last step is critical for the analysis, as each step introduces extraneous carbon, which if not accounted for, could yield biased results. Additional uncertainties, associated with sample collection in the field, were not considered in this study. It should be noted, however, that field blanks have the potential to contribute significantly to the overall uncertainty for ambient aerosol studies (Zotter et al., 2014).

2.1 Isolation of OC and EC

A thermal–optical OC/EC analyzer (Sunset Laboratory Inc.) was used for the combustion and recovery of the OC and EC fractions. The instrument is specifically developed to separate the carbon content of ambient atmospheric samples collected on quartz fiber filters into OC and EC fractions by thermal evaporation and/or oxidation at separate temperature steps. As the carbon fragments pass through a manganese dioxide (MnO_2) oven, they are quantitatively converted to CO_2 gas and measured directly by a self-contained non-dispersive infrared (NDIR) detector system, placed upstream the instrument's outlet. At the end of each run, a known volume of methane (CH_4) is injected into the oven and oxidized to CO_2 to ensure accurate quantification of OC and EC concentrations.

When operated with standard analytical protocols (e.g., NIOSH (NIOSH, 1999), IMPROVE-A (Chow et al., 2007), EUSAAR_2, (Cavalli et al., 2010), the Sunset OC/EC analyzer evaporates the OC fraction under an inert helium (He) atmosphere, while the EC fraction is subsequently oxidized in a He/O_2 mix (Cavalli et al., 2010, Chow et al., 2001). Under these conditions a fraction of the OC can undergo substantial pyrolysis (charring) during the O_2-free step. When measuring concentrations, the amount of charring-derived EC is accounted for internally by the OC/EC analyzer. A tunable diode laser measures the light transmittance of the sample throughout the heating ramp cycle. Since the transmittance decreases as OC is pyrolyzed to EC, but increases as EC and the pyrolyzed OC are removed during the second heating cycle, the OC/EC split point for quantification is defined to be the point at which the laser transmittance returns to its initial value (Bauer et al., 2009). This widely accepted procedure for the determination of OC and EC concentrations may not be suitable for ^{14}C analysis of the EC fraction, especially when analyzing ultra-small samples, because accurate measurements of ^{14}C require a physical separation of the EC from the OC fraction and it is not possible to mathematically correct the ^{14}C data for charring.

For ^{14}C measurements, the Sunset OC/EC analyzer was modified and equipped with a solenoid valve and a gas flow sensor for controlling O_2 flow, which allows the use of pure O_2 (99.999 %) during oxidation (Zhang et al., 2012). The use of pure O_2 reduces OC charring and allows the use of alternative TOA protocols. The O_2 flow is controlled in the same way as the default carrier gases – He (> 99.999 %) and O_2/He mix (10 % O_2 in He) and the reference gas – CH_4 (5 % CH_4 in He), all of which are controlled by the instrument's gas flow program. The gas flow rate through the OC/EC analyzer is adjusted and stabilized at 60 mL min^{-1}.

To achieve a clear physical separation of OC and EC for ^{14}C-based source apportionment, we used the Swiss_4S protocol, which involves four consecutive steps: (S1) pure O_2 at 375 °C for evaporation/oxidation of OC without premature EC evolution, (S2) pure O_2 at 475 °C followed by (S3) in He at 650 °C, both of which aim to achieve complete OC removal before EC isolation and lead to better consistency with TOA protocols like EUSAAR_2, and (S4) pure O_2 at 760 °C for desorption and recovery of EC (Zhang et al., 2012). Note that our analysis differed from the Zhang et al. (2012) method, in which OC is trapped only during (S1). Here, we trapped OC evolving during both (S1) and (S2) to achieve maximum OC recovery. The material evolving during (S3) is defined as a mixture of OC and EC and is not included in the analysis of either carbon fraction and therefore discarded.

Each run was completed by an injection of reference gas (5 % CH_4 in He), allowing for a conversion of sample CO_2-peak sizes to µg C cm^{-2} of sample filter. The OC/EC analyzer is purged with He prior to every run to ensure that there is no cross contamination from a prior run.

During routine operation, fine air particulate matter (PM$_{2.5}$) samples, collected on quartz microfiber filters (Pallflex Tissuquartz, 2500 QAT-UP, Pall, Port Washington, NY) were introduced into the Sunset OC/EC analyzer as 1.5 cm^2 filter punches (dimensions 1 cm × 1.5 cm, Sunset) on a flat quartz spoon. Under the Swiss_4S protocol, separate punches were used for OC and EC analysis. The EC punch

was treated with Milli-Q (MQ) water prior to the analysis to remove the water-soluble OC and minimize charring as follows: a filter disk (23 mm diameter) was placed on a plastic filter holder (25 mm diameter, Sartorius GmbH, Germany) between two sealing rings with the laden side upwards, and 20 mL of MQ water was passed through from the top using a syringe (Zhang et al., 2012). After drying at 60 °C for up to 1 h, a 1.5 cm^2 punch was taken from the disk for analysis.

Standards for calibration of the OC/EC analyzer (e.g., water-soluble OC, such as sucrose) are typically applied as solution, pipetted on a pre-baked filter punch, dried and analyzed through the desired TOA protocol. However, since EC is water insoluble, this procedure cannot be applied when running EC standards for ^{14}C analysis or method verification. To introduce OC and EC reference materials alike, we developed and customized quartz boats (Jelight Company Inc., Irvine, CA, USA), which were placed into a specifically designed round-bowled (instead of flat) quartz spoon (Jelight Company Inc., Irvine, CA, USA). This enabled us to introduce solids into the OC/EC analyzer. Boats were pre-baked at 900 °C for 2 h and stored in a baked, closed porcelain crucible to avoid contamination. Spoons were baked in O$_2$ inside the OC/EC analyzer for 10 min at 920 °C.

2.2   OC/EC-vacuum line

The outlet of the OC/EC analyzer was connected to a vacuum line (Fig. 1), which allows for the physical trapping of the CO$_2$ released during the different steps of the analysis for subsequent ^{14}C measurement. In addition to trapping the CO$_2$ gas, the vacuum line is also used to remove non-condensables and O$_2$. The vacuum line exhibits a very simple design and allows fast and efficient cooling, trapping and release of the gasses. In the following section, all numbers in brackets correspond to the vacuum line parts described in Fig. 1.

Prior to each OC/EC run, the vacuum line was evacuated to 1×10^{-4} torr (0.013 Pa) on the Pirani vacuum gauge (8) using a turbomolecular oil-free diaphragm pump system (9). If no trapping was in progress, the line was kept isolated from the Sunset analyzer and air by keeping valves V2 and V3 closed, while V1 was kept open so the exhaust from the Sunset was open to air (1). The rest of the line stayed open to the turbo pump (9), ensuring the vacuum in the line, which was monitored by both the Pirani vacuum gauge (8) (1×10^{-4} torr at vacuum) and the pressure transducer of the calibrated volume (6) (± 0.1 torr at vacuum). While evacuated, we cleaned the inner surfaces of the break-seal tube (7) of any trapped exogenous C by heating along its length with a blowtorch (O$_2$/natural gas).

Once the Swiss_4S TOA protocol started, the trapping procedure consisted of the following steps: a liquid nitrogen (N$_2$(l)) dewar was placed so it covered the cryogenic trap (2) completely a minute prior to Swiss_4S step (S1)–for OC trapping or (S4)–for EC trapping. The cryogenic trap was

then closed to the pump via V4. When CO$_2$ was evolving from the OC or EC fractions (steps S1 and S2 or S4, respectively), the gas stream was re-directed to the vacuum line by first closing the exhaust (via V1), waiting for the pressure in the line to build to 1 psig (~ 6895 Pa), as shown by the OC/EC analyzer's program, and opening the flow to the cryogenic trap (V2 is opened; pressure drops). After waiting for the pressure to reach 1 psig for a second time, the second exhaust (4) was opened via V3 and stayed open while the Swiss_4S protocol was in progress. During that time, CO$_2$ accumulated in the cryogenic trap. At the end of S2 for OC or S4 for EC, the line was closed off from the OC/EC analyzer. First V3 was closed, and once the pressure again reached 1 psig, V1 was opened and V2 was immediately closed. After this step the CO$_2$ from the desired fraction was in the cryogenic trap. Note that waiting for the pressure to build up before opening the line to either exhaust (1) (at the end of the trapping procedure) or exhaust (4) (at the beginning of the trapping procedure) is crucial in preventing backflow in the system, which could introduce ambient CO$_2$ and O$_2$ from the room air into the N$_2$(l)-cooled sample trap (2). However, the pressure buildup causes the O$_2$ carrier gas to condense in the trap. Once either exhaust is open, the reduced pressure prevents the O$_2$ from condensing in the trap. Releasing the pressure allowed us to avoid the need for an additional chemical trap for O$_2$ trapping, as compared to the setup in Bern.

Next, the O$_2$ that accumulated in the trap during the periods of increased pressure in addition to the sample CO$_2$, was pumped away, together with other non-condensables: N$_2$(l) was left in place (2), while V4 was opened and closed, after which V7 was opened until vacuum was established again. These steps were repeated until the pressure on the pressure gauge (6) was below 300 torr (the upper limit of the pressure transducer) and then the line was finally opened fully to the turbo pump (9). The repeated closing and opening of V4 and V7 was necessary, because the turbo pump cannot operate at high pressures.

After the line pressure at the vacuum gauge (8) was less than 1×10^{-4} torr, the cryogenic trap was closed to the pump via V4, and the N$_2$(l) was replaced with a dry ice–ethanol slurry to release the sample CO$_2$, but not water. The sample was transferred to the calibrated volume (5), where the pressure, corresponding to the carbon mass of the sample, was recorded. Finally, the measured CO$_2$ was transferred to the pre-cleaned 4 mm O.D. Pyrex tube (7) and sealed with the blowtorch for future graphitization and ^{14}C analysis.

2.3   Graphitization and AMS measurements

Our sample CO$_2$ was graphitized and analyzed for its ^{14}C content at the KCCAMS facility. Graphite for AMS measurements is typically produced by reduction of CO$_2$ gas over a catalyst. The production of high quality, uniform graphite targets, suitable for the AMS ion source, is important for the
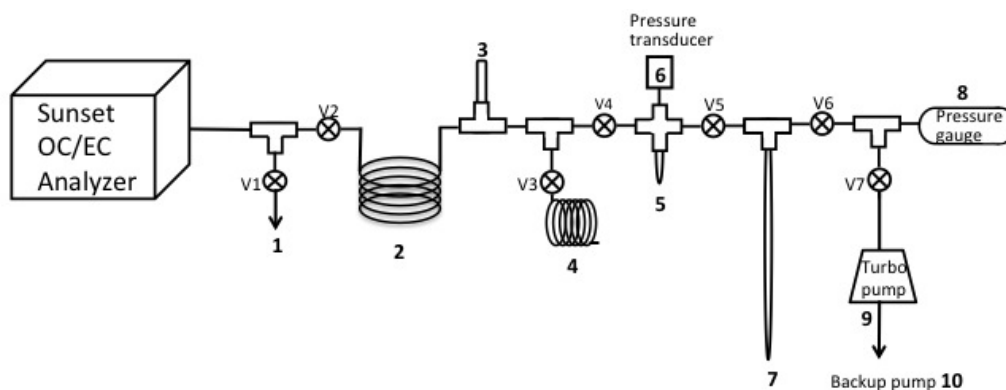
Figure 1. Sunset/Aerosol vacuum line schematic – (1) Exhaust, coming directly from the Sunset – V1 is open whenever trapping is not in progress. (2) Cryogenic trap – allows the evolving CO_2 to accumulate during the trapping procedure, while the trap is submerged in N_2(l). (3) Safety release Pyrex tube – in case of overpressure, this is the point of pressure release. (4) Exhaust during the trapping procedure – the tightly coiled tubing reduces the risk of air flowing inward towards of the vacuum line. (5) Calibrated volume – used to measure the volume of CO_2 trapped. (6) Pressure transducer with metal port (Silicon Microsystems SM5812, 0–5 psi) – monitors the pressure in the calibrated volume. (7) Pyrex break-seal tube – CO_2 is transferred here and sealed off with a torch. (8) Vacuum gauge – monitors the pressure at the end of the line (345 Pirani pressure vacuum sensor, MKS). (9) Turbo Pump (HiPace 80 Turbo-drag Pump, Pfeiffer Vacuum) and (10) Diaphragm pump (MVP 040-2, Pfeiffer Vacuum). The vacuum line is made of 1/8 inch OD, 0.040 inch ID stainless steal tubing and is connected to the outlet of the analyzer. Valves V1–V7 are all Swagelok SS-2P4T valves, 1/8″ stainless steel.

optimal performance of any AMS system. The quality of the graphite influences the level of background contamination, the mass fractionation, and the beam current (Santos et al., 2007c, Kim et al., 2010).

In this study, blanks and standards were chosen to resemble regular fine particulate matter aerosol samples collected over periods of 1–7 days (usually ~ 2–$50\,\mu g$ C) and were much smaller than regular sized ^{14}C samples (~ 300– $1200\,\mu g$ C). A modified protocol was used to maximize yields for our ultra-small samples and to improve target processing and measuring (Santos et al., 2007a). Cryogenically purified CO_2 was transferred into Pyrex tube reactors of $1.6\,cm^3$ volume and reduced to graphite at $450\,°C$ using hydrogen gas over pre-cleaned iron powder as a catalyst. A magnesium perchlorate trap was used to remove water from the reaction. Graphite targets were analyzed for their ^{14}C content using a modified compact AMS system (NEC 0.5 MV 1.5SDH-1) (Beverly et al., 2010).

2.4   Background correction

During the processing of samples for ^{14}C analysis, contamination with extraneous carbon (C_{ex}) always occurs independently of sample size. Its presence can significantly affect the ^{14}C signature of smaller samples and puts a practical lower limit on the minimum ^{14}C sample size that can be reliably measured (Santos et al., 2007a, 2010; Ziolkowski and Druffel, 2009). In some cases, the mass and ^{14}C signature of the C_{ex} can be evaluated directly, and the measured ^{14}C data of unknown samples can be corrected for it, using a mass balance approach. However, when the mass of C_{ex} is too small to directly measure, the extraneous carbon contamina-

tion cannot be quantified using this approach. In this study, we adopted an indirect mathematical approach (Santos et al., 2007a), which treats C_{ex} as a mixture of two components; (a) modern carbon – mostly introduced during sample handling by tools and in equipment, and (b) fossil carbon – originating from ^{14}C-free carbon in the iron powder used to catalyze the reduction of CO_2 to graphite and/or in our OC/EC isolation and trapping setup. The mass of the C_{ex} (m_{ex}) can then be expressed as (Eq. 1):

$$m_{ex} = m_{modern} + m_{fossil}, \tag{1}$$

where m_{modern} is the mass of the modern component and m_{fossil} the mass of the fossil component of C_{ex}.

The average contribution of modern carbon can be quantified by measuring blanks (^{14}C-free materials) of different sizes through each step of the sample processing and is expressed as (Eq. 2):

$$m_{modern} = m_{meas.} \times \frac{FM_{blank}}{FM_{ref}}, \tag{2}$$

where $m_{meas.}$ is the mass measured on the graphitization line, FM_{blank} is the measured ^{14}C signature of the blank, expressed as fraction modern carbon, and FM_{ref} is the fraction modern of a normal-sized, modern reference materials (in this study we used $1\,mg$ C of OX-I). This latter term is directly measured by the AMS system, and reported normalized to six time-bracketed aliquots of the reference material, and corrected for isotope fractionation (Santos et al., 2007b). Similarly, we quantified the average contribution of the fossil component of C_{ex} by measuring the ^{14}C content of modern standards (FM_{std}) with different masses, with known fraction

modern content (Eq. 3):

$$m_{\text{fossil}} = m_{\text{meas.}} \times \frac{[1 - \text{FM}_{\text{std}}]}{\text{FM}_{\text{ref}}}. \tag{3}$$

Finally, the ^{14}C content of a sample can be corrected for the mass and ^{14}C contribution of C_{ex} and expressed as (Eq. 4):

$$\text{FM}_{\text{sample}} = \text{FM}_{\text{cons.}} \times \frac{\left[\dfrac{\text{FM}_{\text{meas.}}}{\text{FM}_{\text{ref}}} - \dfrac{m_{\text{modern}}}{m_{\text{meas.}}}\right]}{\left[1 - \dfrac{m_{\text{modern}}}{m_{\text{meas.}}} - \dfrac{m_{\text{fossil}}}{m_{\text{meas.}}}\right]}, \tag{4}$$

where $\text{FM}_{\text{cons.}}$ is the canonic fraction modern value (the standard multiplier) of the reference material, used to produce the six time-bracketed graphite targets measured in a single batch or wheel, and $\text{FM}_{\text{meas.}}$ is the ^{14}C content of the unknown sample, directly measured by the AMS system. To determine the uncertainty in our calculation of $\text{FM}_{\text{sample}}$, we mathematically propagated the uncertainty, applying a 50 % error in m_{fossil} and m_{modern}, based on long-term measurements of m_{ex} variance in small samples (Santos et al., 2007a). Further detailed description of this approach for correcting ultra-small mass samples and its use at the KCCAMS/UCI can be found in Santos et al. (2007a).

Here, we evaluate the contribution of modern and fossil carbon, introduced both during the TOA analysis with the Swiss_4S on our vacuum line ($C_{\text{swiss\_4S}}$) and during the graphitization procedure (C_{graph}). To assess the overall mass and ^{14}C signature of C_{ex}, we measured a set of blanks and standards through all steps of the analysis for both OC and EC. To quantify the relative contribution of C_{ex} introduced during either processing step, we measured another set of blanks and standards, which only underwent graphitization. The $C_{\text{swiss\_4S}}$ contributions were estimated as the difference between C_{ex} and C_{graph}.

2.5 Materials

To evaluate the mass of the C_{ex} and its associated ^{14}C signature for proper background corrections and to assess the performance of our OC/EC analyzer and vacuum line, we measured a set of ^{14}C fossil (blanks) and modern (standards) reference materials, described in Table 1. They were chosen to have strongly contrasting ^{14}C contents and (when possible) to consist of international reference materials. We chose adipic acid as a blank and oxalic acid (OX-I) as a standard for OC. Coal (POC #3 USGS (United States Geological Survey) coal) and rice char (*Oryza sativa* L.) were used as blank and standard for EC, respectively. Both OC and EC reference materials were introduced into the OC/EC analyzer as solids. The EC reference materials were pre-cleaned using the ABA (acid–base–acid) method (Santos and Ormsby, 2013).

To quantify the efficiency of our setup at trapping each carbon fraction, we measured seven samples with a range of sizes from each reference material, with the exception of OX-I ($n = 6$). For better assessment of the C_{ex} and its ^{14}C content, more samples from the same reference materials were

included from two additional AMS runs. A detailed description of all reference material samples can be found in Appendix A.

A second set of similar-sized ^{14}C reference materials (coal, $n = 2$–4 and OX-I, $n = 3$–5) were graphitized in parallel with each batch of samples (separately for each of the three AMS runs) to quantify any contamination introduced *only* during the graphitization procedure and to distinguish it from the contamination introduced by the OC/EC analyzer and vacuum line.

In addition, we analyzed the ^{14}C content of five mixed OC and EC in ambient particulate matter on quartz fiber filters, which were previously collected and analyzed for their ^{14}C content under the Swiss_4S protocol at the University of Bern, Switzerland. Samples were collected during winter with high-volume air samplers in Switzerland (Bern: 8 January 2009, Chiasso: 11 February 2012, Massongex: 13 February 2012 and Solothurn: 13 February 2012; for details see Zotter et al., 2014) and Poland (Zabrze: Winter 2012) (Appendix B).

3 Results

3.1 Sample recovery

On average, 91 % of the carbon in each sample was cryogenically trapped following the Swiss_4S TOA on the Sunset OC/EC analyzer and attached vacuum line (Fig. 2a). Here, the OC content was directly estimated as the total carbon content of the reference materials, based on its molecular weight. The EC content could only be assessed with our TOA setup, and for each EC run the measured EC content was compared to the average EC content of the reference materials ($n = 7$).

Sample recovery, or yield, during this step reflects the homogeneity of each reference material, the accuracy of weighing samples into the boats, and the efficiency of the cryo-trapping procedures. In general, the OC materials were more pure than the EC materials and consequently showed a better linear relationship between expected and recovered yields (Table 1).

About 5 % of each sample was lost on the graphitization line during the second cryogenic trapping of CO_2 (Fig. 2b). One sample was excluded from this analysis, because only 58 % of sample CO_2 was recovered – implying improper handling. Sample recovery during this step was influenced by CO_2 lost on the break-seal and vacuum line inner surfaces, the efficiency of the cryo-trapping, as well as differences in the calibration of the pressure gauges.

3.2 Background assessment

The amount of C_{ex} introduced during each step of the analysis was estimated indirectly by measuring it as the sum of the modern and fossil ^{14}C background contamination (Table 2).

Table 1. Description of reference materials used for quantifying background contamination and method accuracy of OC and EC trapping and ^{14}C measurements. Parameters of Fig. 2a regard the measured volume vs. expected yield and the coefficient of determination of the linear regression for the individual reference materials as explained in Sect. 3.1.

Standard	Used for	%OC	%EC	Fraction modern	SD	Parameters of Fig. 2a
Oxalic Acid I[a]	OC	19	n/a	1.0399[c] $n = 2618$	0.0021	98 % $R^2 = 0.96$
Adipic Acid	OC	49	n/a	0.0000[e] $n = 5$	0.0002	89 % $R^2 = 0.99$
Rice Char[b]	EC	n/a	2[d]	1.0675[e] $n = 3$	0.0007	86 % $R^2 = 0.90$
Coal	EC	n/a	54[d]	0.0012[c] $n = 300$	0.0004	88 % $R^2 = 0.85$

n/a = not applicable, [a] SRM4990B (National Institute of Standards and Technology, MD, USA), [b] Black carbon reference material (University of Zürich, Switzerland), [c] Beverly et al. (2010), [d] The EC content was estimated by averaging repeated TOA experiments ($n = 7$ for char, $n = 7$ for coal), [e] Repeated measurements of the ^{14}C of the bulk material were performed at the KCCAMS.
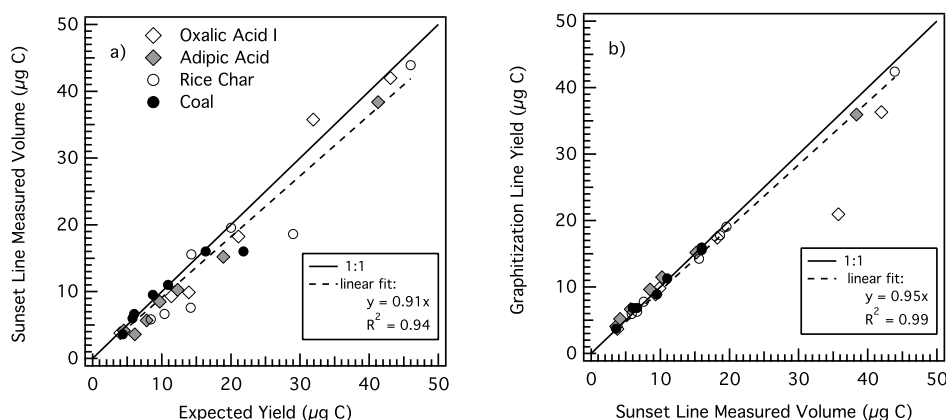

Figure 2. Sample recovery yield at each step of the analysis: **(a)** sample size measured at the calibrated volume of the Sunset vacuum line, compared to expected carbon yield; **(b)** sample size measured on the graphitization line compared to the sample size measured at the Sunset vacuum line.

We found no difference in the amount of C_{ex} introduced during the analysis of OC compared to EC.

The amount of modern carbon introduced during the analysis was $0.8 \pm 0.4 \,\mu g\, C$ (Fig. 3b, d). A comparison of the results for samples that only underwent combustion and graphitization, but not TOA and cryo-trapping, indicated that the Swiss_4S TOA with the OC/EC analyzer plus the attached vacuum line introduced a smaller amount of modern carbon (46 % of modern C_{ex}) than the graphitization procedure (Table 2). Our modern carbon blank estimate was based on the analysis of three separate AMS runs and the exclusion of one coal replicate, which showed an excess modern carbon amount of $1.5 \,\mu g\, C$ and was not comparable to the rest of the blanks.

The total amount of fossil C_{ex} introduced by our method was estimated to be $0.67 \pm 0.34 \,\mu g\, C$ (Fig. 3a, c), primarily (80 % of fossil C_{ex}) due to graphitization, with much smaller contribution from the TOA and the cryo-trapping procedure

(Table 2). Note that to have all ^{14}C results from small reference materials fall within $\pm 2\sigma$ of the expected value, an error of 50 % was then imposed into their background subtractions and propagated into their final uncertainties, as described in Sect. 2.4. This approach accounts for any long-term variability on blank measurements on ultra-small samples, as shown in Santos et al. (2010).

3.3 Intercomparison of aerosol sample ^{14}C measurements

The comparison of ^{14}C measurements of the OC and EC content of PM$_{2.5}$ filter samples at UC Irvine and the University of Bern showed a very good agreement, with samples measured in Bern being slightly enriched in ^{14}C compared to UC Irvine (Fig. 4). A Pearson's major axis type II regression, minimizing both x and y residuals simultaneously with all data given equal weight, showed a strong linear relation with

Table 2. Summary of the amounts and ^{14}C signatures of extraneous carbon introduced during the isolation and graphitization of OC and EC standard materials at UC Irvine.

Source of contamination	Measured contribution µg C	±	Fraction modern equivalent*
Swiss_4S TOA + cryo-trapping			
– modern	0.37	0.18	
– fossil	0.13	0.07	
Total:	0.50	0.25	0.74 ± 0.37
Graphitization			
– modern	0.43	0.22	
– fossil	0.53	0.27	
Total:	0.97	0.48	0.45 ± 0.22
Full setup modern	0.80	0.40	
Full setup fossil	0.67	0.33	
Overall system blank	1.47	0.73	0.55 ± 0.27

* The FM equivalent is calculated by mass balance as: $FM_{ex} = \frac{FM_{modern} \times m_{modern} + FM_{fossil} \times m_{fossil}}{m_{modern} + m_{fossil}}$, with $FM_{modern} \approx 1$ and $FM_{fossil} = 0$.

a slope of 1.24 ± 0.17 and a R^2 value of 0.85. It is worth noting that the EC samples are much smaller in size and consequently have a higher uncertainty level, which can explain the standard deviation of the slope. The steepness of the slope we observed is primarily driven by the smallest measured EC sample, which consequently has highest uncertainty. If this sample is excluded, the new Type II regression slope is equal to 1.07 ± 0.01 and is much closer to the 1 : 1 line with $R^2 = 0.95$.

Further, to obtain a better comparison between the two labs, we performed a paired sample t-test, assuming unequal variances in the measurements of the two labs and two tails. The results showed that the null hypothesis ("means are equal") cannot be rejected at the 5 % significance level for OC, EC and OC and EC together. The p-value or probability of observing the given result was 0.79.

The fraction modern values shown in Fig. 4 were corrected for background contamination during the sample preparation at each lab, but no field blank corrections were applied. This inter-laboratory comparison confirmed that the Swiss_4S TOA protocol can be used successfully with our proposed modifications (cryo-trapping and graphitization procedures) to reproduce OC and EC ^{14}C measurements of unknown aerosol samples.

4 Discussion

The classification of aerosols into OC and EC components is a well-established paradigm, but the split point is not clearly defined and highly dependent on the separation procedure. Therefore, our ability to quantitatively measure and apportion OC and EC is method-specific (Currie et al., 2002). The TOA protocols used to measure OC and EC in partic-

ulate matter by mass can only be mathematically corrected for charring (e.g., IMPROVE_A). However, a TOA protocol allowing for the isolation of OC and EC for accurate ^{14}C measurements, especially for ultra-small samples, requires a complete *physical* removal of interfering fractions with maximum recovery of each fraction. This is largely because the OC and EC fractions differ in their ^{14}C signature and charring would transfer OC with an unknown ^{14}C signature into the EC fraction and thus change the ^{14}C signature of both fractions. Our results confirmed that the Swiss_4S protocol successfully isolates OC and EC with very different ^{14}C contents when implemented in a new laboratory setting. We obtained high yields and reproducible and accurate ^{14}C measurements of both the OC and EC fractions.

We were further able to successfully quantify the amount and ^{14}C signature of the extraneous carbon (C_{ex}) introduced during each step of the analysis, and apply appropriate corrections. For the OC fraction, we chose to combine the first two steps S1 and S2 of the Swiss_4S protocol to ensure complete OC recovery. It is important to note that this modification to the Swiss_4S protocol increases the trapping time and thus the probability for trapping prematurely evolving EC. The results from the comparison between Bern and UC Irvine show that there is no detectable difference in the ^{14}C measurements of OC when OC is trapped at both S1 and S2 (UC Irvine) or S1 only (University of Bern). However, our estimate for the blanks of the system based on the OC data is therefore an upper limit of the blank due to the S2 extension and could potentially be reduced if OC trapping is only done during S1.

The EC reference materials (coal and rice char) used for quantifying the background were introduced into the OC/EC analyzer as solids and unlike regular EC filter samples, they
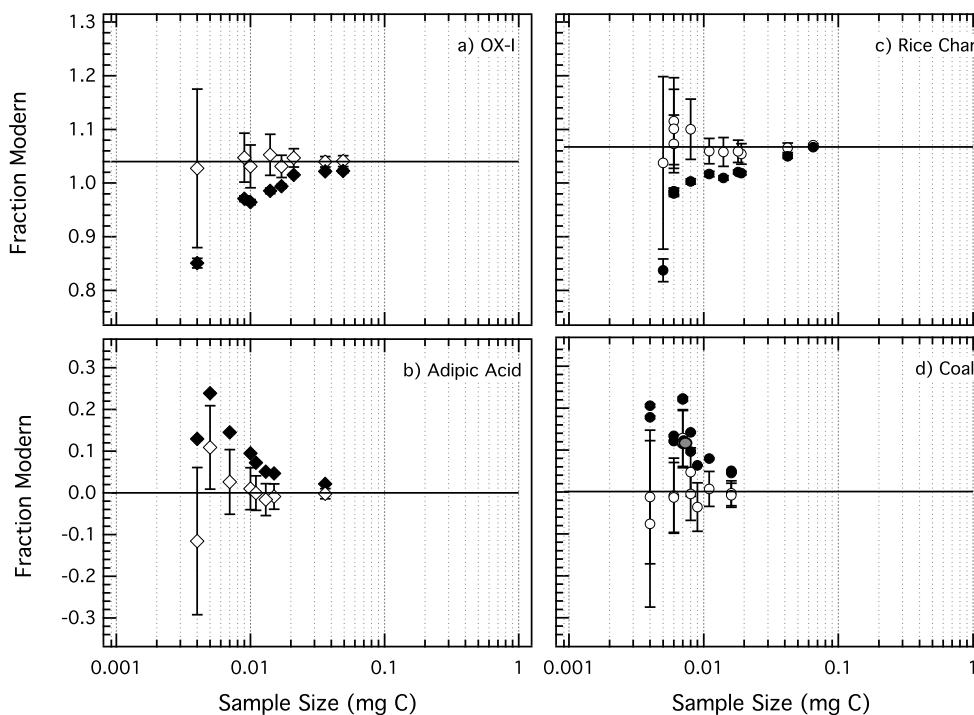
Figure 3. Background correction for OC standards (left panels: **(a)** OX-I and **(b)** adipic acid) and EC standards (right panels: **(c)** rice char and **(d)** coal). Black symbols represent the measured ^{14}C content of each standard prior to background correction. The white symbols show the ^{14}C content for each standard after background correction was applied. Horizontal lines show the consensus ^{14}C content, expressed as fraction modern (f_M) for each standard. The top panels show the modern reference materials used to quantify the fossil contamination, while the bottom panels show the ^{14}C-free blanks used to quantify the modern contamination. Note that the gray circle in panel **(d)** represents a coal sample after background correction, which was excluded from the calculation of the modern blank as an outlier.
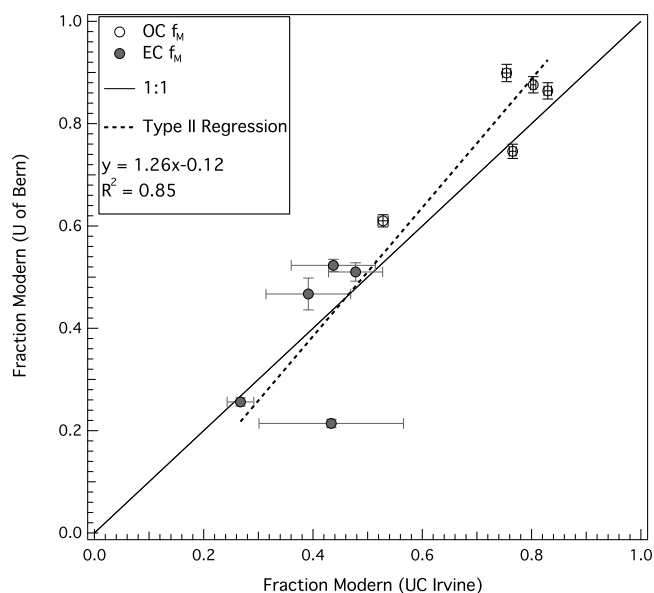

Figure 4. Intercomparison between ^{14}C measurements of OC and EC on five $PM_{2.5}$ filters, measured at the University of Bern and the University of California, Irvine.

did not undergo water extraction pretreatment, which could allow for water soluble gas or particles to attach to the EC surface. This could contaminate the EC measurement with small but dateable amount and means that the EC blanks estimated here are also an upper limit of the EC blank.

The modern carbon blank of the graphitization procedure measured in this study is in good agreement with a previous estimate (0.2–1 µg C) for ultra-small samples at the KC-CAMS facility (Santos et al., 2007a). The fossil carbon contamination expected at the KCCAMS is 0.1–0.5 µg C (Santos et al., 2007a), which is slightly lower than what we measured. By quantifying the background corrections necessary at each step of the procedure, we are now in a position to accurately track any C_{ex} introduced through the procedure and correct for it when interpreting ^{14}C measurements of environmental samples. It is important to note that the C_{ex} analysis described here should be carried out in parallel with each batch of ambient samples, as it is affected by the performance of the AMS system (Santos et al., 2007a).

The modern and fossil contributions of C_{ex} for the Swiss_4S TOA and cryo-trapping corresponded to an overall C_{ex} of 0.55 ± 0.27 µg C with a FM of 0.74 ± 0.37 at UC Irvine. This value is similar to measurements made in Bern (0.4 ± 0.2 µg C with a FM of 0.76 ± 0.17) that were obtained

from a simplified aerosol system (Jenk et al., 2007) and used for background correction of the Bern results shown here.

5 Conclusions

We used an OC/EC analyzer in a new laboratory setting to quantify the precision and accuracy of OC and EC ^{14}C measurements with the Swiss_4S TOA protocol. A set of OC and EC ^{14}C reference materials, blanks and intercomparison samples, with sizes as small as 4 µg C, were analyzed to evaluate the performance of our analytical setup, quantify the uncertainties, and compare the consistency of our results for a shared set of ambient air samples from another laboratory. We were able to do the following: (1) successfully separate OC and EC fractions with the Swiss_4S protocol, (2) isolate and trap the different fractions with our newly developed setup with high yields and low carbon blanks, and (3) measure precisely the ^{14}C content of the separate fractions by quantifying and correcting for contamination at each set of the analysis. Our results were in good agreement with ^{14}C measurements from the Laboratory of Radiochemistry and Environmental Chemistry at the University of Bern.

This is the first study incorporating ^{14}C standard materials to track and quantify background carbon introduced during aerosol OC and EC ^{14}C analysis. In general, the OC and EC contents of an aerosol sample are on the order of a few micrograms (the size of typical EC sample) to tens of micrograms (the size of typical OC sample). Therefore, not accounting for the extraneous carbon introduced during the analysis can significantly bias the results. This is particularly important for the ^{14}C measurements of the typically smaller EC fraction. For ambient aerosol studies, the correction of field blanks will also be very important.

The most recent intercomparison of ^{14}C analysis of carbonaceous aerosols concluded that it is not possible to agree on common procedures of OC and EC isolation among the participating labs, and that an overarching laboratory and method intercomparison quantifying both the concentration and ^{14}C content of OC and EC is still needed (Szidat et al., 2013). Our study presents a first step towards the development of a common protocol for OC and EC ^{14}C measurements.

Appendix A: List of standard and blank samples

Table A1. Radiocarbon measurements of reference materials with a known fraction modern value (standards). The table includes the results both *after* and *before* background correction.

UCI AMS#	Size (µg C)	Fraction modern	Δ^{14}C (‰)	Fraction modern *uncorrected*	Δ^{14}C (‰) *uncorrected*
OC (OX-I)					
125 945	9.81	1.031 ± 0.040	23 ± 40	0.964 ± 0.005	-43 ± 5
125 946	8.89	1.047 ± 0.046	39 ± 46	0.971 ± 0.005	-36 ± 5
125 947	17.41	1.031 ± 0.021	24 ± 21	0.994 ± 0.004	-13 ± 4
125 948	20.93	1.047 ± 0.017	39 ± 17	1.015 ± 0.003	8 ± 3
125 949	36.3	1.040 ± 0.010	32 ± 10	1.022 ± 0.003	14 ± 3
125 950	3.7	1.027 ± 0.148	20 ± 148	0.851 ± 0.009	-156 ± 9
130 366*	49.26	1.041 ± 0.010	33 ± 10	1.023 ± 0.004	15 ± 4
130 368*	14.07	1.053 ± 0.038	45 ± 38	0.986 ± 0.005	-22 ± 5
EC (Rice Char)					
125 951	14.26	1.058 ± 0.027	50 ± 27	1.009 ± 0.004	2 ± 4
125 952	5.93	1.115 ± 0.081	107 ± 81	0.984 ± 0.006	-24 ± 7
125 953	6.3	1.101 ± 0.074	93 ± 74	0.981 ± 0.006	-27 ± 6
125954	7.78	1.100 ± 0.056	92 ± 56	1.003 ± 0.005	-5 ± 5
125 955	19.07	1.054 ± 0.019	46 ± 19	1.019 ± 0.003	11 ± 3
125 956	17.78	1.059 ± 0.021	51 ± 21	1.020 ± 0.004	13 ± 4
125 957	42.41	1.066 ± 0.009	58 ± 9	1.050 ± 0.004	42 ± 4
130 371*	4.63	1.038 ± 0.160	30 ± 161	0.837 ± 0.021	-169 ± 21
132 134*	11.48	1.059 ± 0.024	51 ± 24	1.017 ± 0.005	9 ± 5
132 135*	5.74	1.073 ± 0.054	65 ± 54	0.985 ± 0.006	-23 ± 6
132 139*	65.00	1.071 ± 0.003	63 ± 3	1.067 ± 0.002	59 ± 2

* denotes standards and blanks, which were used only as a radiocarbon reference material during different AMS runs and are not part of the Swiss_4S yield analysis.

Table A2. Radiocarbon measurements of ^{14}C free materials (blanks). Following conventional AMS data reporting, blanks are not corrected for background contamination.

UCI AMS#	Size (µg C)	Fraction modern *uncorrected*	Δ^{14}C (‰) *uncorrected*
OC (Adipic acid)			
125 958	4.07	0.130 ± 0.003	-871 ± 3
125 959	6.67	0.145 ± 0.003	-856 ± 3
125 960	5.19	0.239 ± 0.003	-763 ± 3
125 961	9.63	0.095 ± 0.002	-906 ± 2
125 962	11.48	0.072 ± 0.002	-928 ± 2
125 963	15.19	0.047 ± 0.001	-954 ± 1
125 964	35.93	0.021 ± 0.000	-979 ± 0
130 369[a]	12.78	0.051 ± 0.001	-949 ± 1
EC (Coal)			
125 965	3.7	0.178 ± 0.003	-823 ± 3
125 966	8.89	0.064 ± 0.001	-937 ± 1
125 967	6.85	0.221 ± 0.005	-781 ± 5
125 968	11.3	0.080 ± 0.002	-921 ± 2
125 969	15.56	0.050 ± 0.001	-950 ± 1
125 970	15.93	0.045 ± 0.001	-955 ± 1
125 971	6.85	0.223 ± 0.004	-779 ± 4
130 367[b]	6.85	0.402 ± 0.008	-601 ± 8
130 370[a]	8.33	0.096 ± 0.003	-905 ± 3
132 133[a]	5.93	0.134 ± 0.002	-867 ± 3
132 136[a]	3.89	0.206 ± 0.004	-796 ± 4
132 137[a]	8.15	0.142 ± 0.002	-859 ± 2
132 138[a]	6.30	0.122 ± 0.002	-879 ± 2

[a] denotes standards and blanks, which were used only as a radiocarbon reference material during different AMS runs and are not part of the Swiss_4S yield analysis. [b] was excluded from the blank assessment as an outlier.

Appendix B: Intercomparison samples

Table B1. KCCAMS analysis of intercomparison samples after background correction.

UCI AMS#	Size (µg C)	Fraction modern	Δ^{14}C (‰)
OC samples			
130 356	37.41	0.528 ± 0.009	-476 ± 9
130 357	49.44	0.754 ± 0.008	-252 ± 8
130 358	55.37	0.830 ± 0.007	-177 ± 7
130 359	83.33	0.803 ± 0.005	-203 ± 5
130 360	65.37	0.765 ± 0.006	-241 ± 6
EC samples			
130 361	15.37	0.267 ± 0.024	-735 ± 24
130 362	4.00	0.434 ± 0.132	-570 ± 132
130 363	5.74	0.437 ± 0.077	-566 ± 77
130 364	5.74	0.391 ± 0.078	-612 ± 78
130 365	7.96	0.478 ± 0.050	-526 ± 50

References

Ammann, M., Kalberer, M., Jost, D., and Tobler, L.: Heterogeneous production of nitrous acid on soot in polluted air masses, Nature, 215, 157–160, 1998.

Andreae, M. O. and Gelencsér, A.: Black carbon or brown carbon? The nature of light-absorbing carbonaceous aerosols, Atmos. Chem. Phys., 6, 3131–3148, doi:10.5194/acp-6-3131-2006, 2006.

Bauer, J. J., Yu, X.-Y., Cary, R., Laulainen, N., and Berkowitz, C.: Characterization of the Sunset Semi-Continuous Carbon Aerosol Analyzer, J. Air Waste Manage. Assoc., 59, 826–833, 2009.

Beverly, R., Beaumont, W., Tauz, D., Ormsby, K. M., Reden, K. F., Santos, G. M., and Southon, J. R.: The Keck Carbon Cycle AMS Laboratory, University of California, Irvine: status report, Radiocarbon, 52, 301–309, 2010.

Bond, T. C., Doherty, S. J., Fahey, D. W., Forster, P. M., Berntsen, T., DeAngelo, B. J., Flanner, M. G., Ghan, S., Kärcher, B., Koch, D., Kinne, S., Kondo, Y., Quinn, P. K., Sarofim, M. C., Schultz, M. G., Schulz, M., Venkataraman, C., Zhang, H., Zhang, S., Bellouin, N., Guttikunda, S. K., Hopke, P. K., Jacobson, M. Z., Kaiser, J. W., Klimont, Z., Lohmann, U., Schwarz, J. P., Shindell, D., Storelvmo, T., Warren, S. G., and Zender, C. S.: Bounding the role of black carbon in the climate system: A scientific assessment, J. Geophys. Res. Atmos., 118, 5380–5552, 2013.

Cavalli, F., Viana, M., Yttri, K. E., Genberg, J., and Putaud, J.-P.: Toward a standardised thermal-optical protocol for measuring atmospheric organic and elemental carbon: the EUSAAR protocol, Atmos. Meas. Tech., 3, 79–89, doi:10.5194/amt-3-79-2010, 2010.

Chow, J. C., Watson, J. G., Crow, D., Lowenthal, D. H., and Merrifield, T.: Comparison of IMPROVE and NIOSH Carbon Measurements, Aerosol Sci. Technol., 34, 23–34, 2001.

Chow, J. C., Watson, J. G., Chen, L. W. A., Arnott, W. P., Moosmüller, H., and Fung, K.: Equivalence of elemental carbon by thermal/optical reflectance and transmittance with different temperature protocols, Environ. Sci. Technol., 38, 4414–4422, 2004.

Chow, J. C., Watson, J. G., Chen, L. W. A., Chang, M. C. O., Robinson, N. F., Trimble, D., and Kohl, S.: The IMPROVE_A temperature protocol for thermal/optical carbon analysis: maintaining consistency with a long-term database., J. Air Waste Manag. Assoc., 57, 1014–1023, 2007.

Clayton, G. D., Arnold, J. R., and Patty, F. A.: Determination of sources of particulate atmospheric carbon, Science 122, 751–753, 1955.

Currie, L. A., Benner, B. A., Kessler, J. D., Klinedinst, B. D., Klouda,, G. A., Marolf, J. V., Slater, J. F., Wise, S. A., Cachier, H., Cary, R., Chow, J.C., Watson, J., Druffel, E. R. M., Masiello, C. A., Eglinton, T. I., Pearson, A., Reddy, C. M., Gustafsson, O., Quinn, J. G., Hartmann, P. C., Hedges, J. I., Prentice, K. M.,

Kirchstetter, T. W., Novakov, T., Puxbaum, H., Schmid, H.: A critical evaluation of interlaboratory data on total, elemental, and isotopic carbon in the carbonaceous particle reference material, NIST SRM 1649a, J. Res. Natl. Inst. Stan., 107, 279–298, 2002.

Dusek, U., Reischl, G. P., and Hitzenberger, R.: CCN activation of pure and coated carbon black particles, Environ. Sci. Technol., 40, 1223–1230, 2006.

Gauderman, W. and Avol, E.: The Effect of Air Pollution on Lung Development from 10 to 18 Years of Age, N. Engl. J. Med., 351, 1057–1067, 2004.

Griffin, J. and Goldberg, E.: Notes. Impact of fossil fuel combustion on sediments of Lake Michigan: a reprise, Environ. Sci. Technol., 17, 244–245, 1983.

Hallquist, M., Wenger, J. C., Baltensperger, U., Rudich, Y., Simpson, D., Claeys, M., Dommen, J., Donahue, N. M., George, C., Goldstein, A. H., Hamilton, J. F., Herrmann, H., Hoffmann, T., Iinuma, Y., Jang, M., Jenkin, M. E., Jimenez, J. L., Kiendler-Scharr, A., Maenhaut, W., McFiggans, G., Mentel, Th. F., Monod, A., Prévôt, A. S. H., Seinfeld, J. H., Surratt, J. D., Szmigielski, R., and Wildt, J.: The formation, properties and impact of secondary organic aerosol: current and emerging issues, Atmos. Chem. Phys., 9, 5155–5236, doi:10.5194/acp-9-5155-2009, 2009.

Janssen, N. A. H., Hoek, G., Simic-Lawson, M., Fischer, P., Bree, L. Van, Brink, H., Keuken, M., Atkinson, R. W., Anderson, H. R., Brunekreef, B., and Cassee, F. R.: Review Black Carbon as an Additional Indicator of the Adverse Health Effects of Airborne Particles Compared with PM_{10} and $PM_{2.5}$, Environ. Health Perspect., 12, 1691–1699, 2011.

Jenk, T. M., Szidat, S. Schwikowski, M., Gäggeler, H. W., Wacker, L., Synal, H.-A., and Saurer, M., Microgram level radiocarbon (^{14}C) determination on carbonaceous particles in ice, Nucl. Instrum. Meth. Phys. Res. B, 259, 518–525, 2007.

Jimenez, J. L., Canagaratna, M. R., Donahue, N. M., Prevot, a S. H., Zhang, Q., Kroll, J. H., DeCarlo, P. F., Allan, J. D., Coe, H., Ng, N. L., Aiken, a C., Docherty, K. S., Ulbrich, I. M., Grieshop, a P., Robinson, a L., Duplissy, J., Smith, J. D., Wilson, K. R., Lanz, V. a, Hueglin, C., Sun, Y. L., Tian, J., Laaksonen, a, Raatikainen, T., Rautiainen, J., Vaattovaara, P., Ehn, M., Kulmala, M., Tomlinson, J. M., Collins, D. R., Cubison, M. J., Dunlea, E. J., Huffman, J. a, Onasch, T. B., Alfarra, M. R., Williams, P. I., Bower, K., Kondo, Y., Schneider, J., Drewnick, F., Borrmann, S., Weimer, S., Demerjian, K., Salcedo, D., Cottrell, L., Griffin, R., Takami, a, Miyoshi, T., Hatakeyama, S., Shimono, a, Sun, J. Y., Zhang, Y. M., Dzepina, K., Kimmel, J. R., Sueper, D., Jayne, J. T., Herndon, S. C., Trimborn, a M., Williams, L. R., Wood, E. C., Middlebrook, a M., Kolb, C. E., Baltensperger, U., and Worsnop, D. R.: Evolution of organic aerosols in the atmosphere, Science, 326, 1525–1529, 2009.

Johnston, F. H., Henderson, S. B., Chen, Y., Randerson, J. T., Marlier, M., Defries, R. S., Kinney, P., Bowman, D. M. J. S., and Brauer, M.: Estimated global mortality attributable to smoke from landscape fires, Environ. Health Perspect., 120, 695–701, 2012.

Kim, S.-H., Kelly, P. B., Ortalan, V., Browning, N. D., and Clifford, A. J.: Quality of graphite target for biological/biomedical/environmental applications of 14C-accelerator mass spectrometry, Anal. Chem., 82, 2243–2252, 2010.

Lary, D., Lee, A., Toumi, R., Newchurch, M. J., Pirre, M., and Renard, J. B.: Carbon aerosols and atmospheric photochemistry, J. Geophys. Res., 102, 3671–3682, 1997.

Levin, I., Naegler, T., Kromer, B., Diehl, M., Francey, R. J., Gomez-Pelaez, A. J., Steele, L. P., Wagenbach, D., Weller, R., and Worthy, D. E.: Observations and modelling of the global distribution and long-term trend of atmospheric $^{14}CO_2$, Tellus B, 62, 26–46, 2010.

Mauderly, J. and Chow, J.: Health effects of organic aerosols, Inhal. Toxicol., 20, 257–288, 2008.

McConnell, J. R., Edwards, R., Kok, G. L., Flanner, M. G., Zender, C. S., Saltzman, E. S., Banta, J. R., Pasteris, D. R., Carter, M. M., and Kahl, J. D. W.: 20th-century industrial black carbon emissions altered Arctic climate forcing, Science, 317, 1381–1384, 2007.

NIOSH: ELEMENTAL CARBON (DIESEL PARTICULATE): METHOD 5040, in Manual of Analytical Methods, National Institute of Occupational Safety and Health, Cincinnati, OH, 1–9, 1999.

Novakov, T. and Penner, J.: Large contribution of organic aerosols to cloud-condensation-nuclei concentrations, Nature, 365, 823–826 1993.

Penner, J. E., Prather, M. J., Isaksen, I. S. a., Fuglestvedt, J. S., Klimont, Z., and Stevenson, D. S.: Short-lived uncertainty?, Nat. Geosci., 3, 587–588, 2010.

Pöschl, U.: Atmospheric aerosols: composition, transformation, climate and health effects, Angew. Chem. Int. Ed. Engl., 44, 7520–7540, 2005.

Santos, G. M. and Ormsby, K. M.: Behavioral variability in ABA chemical pretreatment close to the ^{14}C age limit, Radiocarbon, 55, 534–544, 2013.

Santos, G. M., Southon, J. R., Griffin, S., Beaupre, S. R., and Druffel, E. R. M.: Ultra small-mass AMS 14C sample preparation and analyses at KCCAMS/UCI Facility, Nucl. Instrum. Meth. Phys. Res. B, 259, 293–302, 2007a.

Santos, G. M., Moore, R., Southon, J., Griffin, S., Hinger, E., and Zhang, D.: AMS 14C Preparation at the KCCAMS/UCI Facility: status REPORT AND PERFORMANCE OF SMALL SAMPLES, Radiocarbon, 49, 255–269, 2007b.

Santos, G. M., Mazon, M., Southon, J. R., Rifai, S., and Moore, R. Evaluation of iron and cobalt powders as catalysts for 14C-AMS target preparation, Nucl. Instrum. Meth. Phys. Res. B, 259, 308–315, 2007c.

Santos, G. M., Southon, J. R., Drenzek, N. J., Ziolkowski, L. A., Druffel, E., Xu, X., Zhang, D., Trumbore, S., Eglinton, T. I., and Hughen, K. A.: Blank assessment for ultra-small radiocarbon samples, Radiocarbon, 52, 1322–1335, 2010.

Schauer, J. J., Mader, B. T., Deminter, J. T., Heidemann, G., Bae, M. S., Seinfeld, J. H., Flagan, R. C., Cary, R. a, Smith, D., Huebert, B. J., Bertram, T., Howell, S., Kline, J. T., Quinn, P., Bates, T., Turpin, B., Lim, H. J., Yu, J. Z., Yang, H., and Keywood, M. D.: ACE-Asia intercomparison of a thermal-optical method for the determination of particle-phase organic and elemental carbon., Environ. Sci. Technol., 37, 993–1001, 2003.

Schmid, H., Laskus, L., Abraham, H. J., Baltensperger, U., Lavanchy, V., Bizjak, M., Burba, P., Cachier, H., Crow, D., Chow, J. C., Gnauk, T., Even, A., Brink, H., Giesen, K., Hitzenberg, R., Hueglin, C., Maenhaut, W., Pio, C., Carvalho, A., Putaud, J., Toom-Sauntry, T., and Puxbaum, H.: Results of the "carbon conference" international aerosol carbon round robin test stage I, Atmos. Environ., 35, 2111–2121, 2001.

Spracklen, D. V., Carslaw, K. S., Pöschl, U., Rap, A., and Forster, P. M.: Global cloud condensation nuclei influenced by carbonaceous combustion aerosol, Atmos. Chem. Phys., 11, 9067–9087, doi:10.5194/acp-11-9067-2011, 2011.

Szidat, S., Jenk, T. M., Gäggeler, H. W., Synal, H.–A., Fisseha, R., Baltensperger, U., Kalberer, M., Samburova, V., Reimann, S., Kasper-Giebl, A., and Hajdas, I.: Radiocarbon (^{14}C)-deduced biogenic and anthropogenic contributions to organic carbon (OC) of urban aerosols from Zürich, Switzerland, Atmos. Environ., 38, 4035–4044, 2004.

Szidat, S., Ruff, M., Perron, N., Wacker, L., Synal, H.-A., Hallquist, M., Shannigrahi, A. S., Yttri, K. E., Dye, C., and Simpson, D.: Fossil and non-fossil sources of organic carbon (OC) and elemental carbon (EC) in Göteborg, Sweden, Atmos. Chem. Phys., 9, 1521–1535, doi:10.5194/acp-9-1521-2009, 2009.

Szidat, S., Bench, G., Bernardoni, V., Calzolai, G., Czimczik, C. I., Derendorp, L., Dusek, U., Elder, K., Fedi, M. E., Genberg, J., Gustafsson, O., Kirillova, E., Kondo, M., McNichol, A., Perron, N., Santos, G. M., Stenström, K., Swietlicki, E., Uchida, M., Vecchi, R., Wacker, L., Zhang, Y. L., and Prévôt, A. S. H.: ^{14}C analysis of carbonaceous aerosols?: Exercise 2009, Radiocarbon, 55, 1496–1509, 2013.

Zhang, Y. L., Perron, N., Ciobanu, V. G., Zotter, P., Minguillón, M. C., Wacker, L., Prévôt, A. S. H., Baltensperger, U., and Szidat, S.: On the isolation of OC and EC and the optimal strategy of radiocarbon-based source apportionment of carbonaceous aerosols, Atmos. Chem. Phys., 12, 10841–10856, doi:10.5194/acp-12-10841-2012, 2012.

Ziolkowski, L. and Druffel, E.: Quantification of extraneous carbon during compound specific radiocarbon analysis of black carbon, Anal. Chem., 81, 10156–10161, 2009.

Zotter, P., Ciobanu, V. G., Zhang, Y. L., El-Haddad, I., Macchia, M., Daellenbach, K. R., Salazar, G. A., Huang, R.-J., Wacker, L., Hueglin, C., Piazzalunga, A., Fermo, P., Schwikowski, M., Baltensperger, U., Szidat, S., and Prévôt, A. S. H.: Radiocarbon analysis of elemental and organic carbon in Switzerland during winter-smog episodes from 2008 to 2012 –Part 1: Source apportionment and spatial variability, Atmos. Chem. Phys., 14, 13551–13570, doi:10.5194/acp-14-13551-2014, 2014.